



Original Article

A 3-Layered Bioartificial Blood Vessel with Physiological Wall Architecture Generated by Mechanical Stimulation

FLORIAN HELMS ¹, SKADI LAU,¹ THOMAS APER,^{1,2} SARAH ZIPPUSCH,¹
MELANIE KLINGENBERG,¹ AXEL HAVERICH,^{1,2} MATHIAS WILHELMI,^{1,3}
and ULRIKE BÖER^{1,2}

¹Lower Saxony Centre for Biomedical Engineering, Implant Research and Development (NIFE), Hannover Medical School, Stadtfelddamm 34, 30625 Hannover, Germany; ²Division for Cardiothoracic-, Transplantation- and Vascular Surgery, Hannover Medical School, Hannover, Germany; and ³Department of Vascular- and Endovascular Surgery, St. Bernward Hospital, Hildesheim, Germany

(Received 2 November 2020; accepted 6 January 2021; published online 22 January 2021)

Associate Editor Smadar Cohen oversaw the review of this article.

Abstract—The generation of cellularized bioartificial blood vessels resembling all three layers of the natural vessel wall with physiological morphology and cell alignment is a long pursued goal in vascular tissue engineering. Simultaneous culture of all three layers under physiological mechanical conditions requires highly sophisticated perfusion techniques and still today remains a key challenge. Here, three-layered bioartificial vessels based on fibrin matrices were generated using a stepwise molding technique. Adipose-derived stem cells (ASC) were differentiated to smooth muscle cells (SMC) and integrated in a compacted tubular fibrin matrix to resemble the *tunica media*. The *tunica adventitia*-equivalent containing human umbilical vein endothelial cells (HUVEC) and ASC in a low concentration fibrin matrix was molded around it. Luminal seeding with HUVEC resembled the *tunica intima*. Subsequently, constructs were exposed to physiological mechanical stimulation in a pulsatile bioreactor for 72 h. Compared to statically incubated controls, mechanical stimulation induced physiological cell alignment in each layer: Luminal endothelial cells showed longitudinal alignment, cells in the *media*-layer were aligned circumferentially and expressed characteristic SMC marker proteins. HUVEC in the *adventitia*-layer formed longitudinally aligned microvascular tubes resembling *vasa vasorum* capillaries. Thus, physiologically organized three-layered bioartificial vessels were successfully manufactured by stepwise fibrin molding with subsequent mechanical stimulation.

Keywords—Bioreactor technique, Perfusion system, Pulsatile perfusion, Flow conditioning, Vascular tissue engineering, Vascular graft, Fibrin matrix.

INTRODUCTION

Cardiovascular diseases are the number one cause of death worldwide.⁵ Within this spectrum, vasculopathies of small caliber arteries (< 5 mm in diameter) represent a surgically challenging etiology and cause a decisive part of morbidity and mortality in industrialized countries. In current clinical practice, vascular prostheses made of alloplastic materials are commonly used for replacing or bypassing diseased natural vessels. Although larger diameter synthetic grafts have been used for decades with good clinical results, insufficient biocompatibility of alloplastic graft materials causes complications such as graft occlusion by thrombosis or inflammatory processes, which is especially problematic in small diameter prostheses. Thus, there is an ongoing need for innovations in the field of vascular prostheses especially for uses in small diameter vasculature. For this application, innovative vascular grafts must meet distinctively higher requirements concerning hemo- and biocompatibility than current options. Vascular tissue engineering has emerged as a promising approach to maximize biocompatibility of vascular grafts by creating bioartificial vessels, which mimic the structure of natural blood vessels as accurately as possible. Generation of small

Address correspondence to Florian Helms, Lower Saxony Centre for Biomedical Engineering, Implant Research and Development (NIFE), Hannover Medical School, Stadtfelddamm 34, 30625 Hannover, Germany. Electronic mail: helms.florian@mh-hannover.de

caliber bioartificial vessels with physiological morphology and function requires the combination of suitable matrix materials and specific cell types with physiological cell alignment. While promising advances in the generation of functional bioartificial vessels using tissue engineering techniques have been achieved,¹⁷ resembling all layers of the physiological arterial wall in an *in vitro* cellularized tissue engineered vascular prosthesis optimizes the emulation of the natural vessel wall structure and thus, potentially increases biocompatibility.

Human blood vessel walls physiologically consist of three layers: The *tunica intima* built up by endothelial cells, the *tunica media* with vascular smooth muscle cells and the *tunica adventitia*. Besides collagen producing fibroblasts and myofibroblasts, autonomic nerves and lymphatic vessels, this layer contains a dense capillary network emerging from the so called *vasa vasorum* which facilitate nutrition of the vessel wall.

First prerequisite for the generation of cellularized bioartificial vessels resembling all three layers of the vessel wall is to obtain the different cell types needed and to identify or generate a matrix suitable for luminal and intramural cell seeding and capillary tube formation. In addition to that, the components have to be arranged in a physiologically layered fashion. Within each layer, proper cell morphology and orientation is needed to comply with the physiological arrangement of native arteries. In order to accurately resemble the complex structure of the vessel wall, a tissue engineering strategy combining specific techniques for each layer is needed.

As one of these techniques, mechanical stimulation in pulsatile bioreactor perfusion systems (BPS) has been shown to be of pivotal importance not only for mesenchymal stem cell differentiation towards vascular smooth muscle cells⁸ but also for proper alignment and function of both, mural smooth muscle cells and luminal endothelial cells.¹¹ Application of physiological mechanical stimuli to multi-layered bioartificial vessels requires highly sophisticated techniques for vascular construct generation and bioreactor design. This represents a limitation that has not yet been sufficiently overcome.

Previous works have focused on generating single layered bioartificial vessels of either the *tunica intima* or the *tunica media* or combining both layers to generate bi-layered vessels.²² Recent attempts for the generation of three-layered vessels including a *tunica adventitia*-equivalent focus on extracellular matrix production by seeding with fibroblasts rather than capillarization of the adventitial layer.^{18,32} Another approach is based on the generation of acellular three-layered matrices resembling stiffness properties of each

layer,³³ which are implanted and subsequently cellularized in the target organism.⁴ Until now, only very few studies have targeted *in vitro* capillarization of the *tunica adventitia*.⁶ Furthermore, a completely cellularized bioartificial vessel that includes a capillarized *tunica adventitia*-equivalent and resembles the physiological hierarchical arrangement of all three layers of the vascular wall with their specific cell orientation and morphology has not been generated *in vitro* yet.

Here, we present the generation of a cellularized three-layered bioartificial vessel built up on a fibrin-based matrix and containing a bioengineered *tunica intima* resembled by a luminal layer of human umbilical vein endothelial cells (HUVEC), a *tunica media*-equivalent built up by vascular smooth muscle cells (SMC), which are differentiated from adipose-derived stem cells (ASC), and a *tunica adventitia*-equivalent that contains a capillary network formed by HUVEC and ASC. Subsequently, the role of mechanical stimulation for cell distribution, differentiation, morphology and alignment was evaluated by comparing three-layered vessels stimulated under physiological conditions in a pulsatile BPS to statically incubated controls.

MATERIALS AND METHODS

Three-Layered Fibrin Vessel Fabrication

A total of six three-layered fibrin based small diameter bioartificial vessels were generated using a four step approach (Fig. 1):

In the first step, the *tunica media*-equivalent was fabricated (Fig. 1-1). Therefore, ASCs were isolated from subcutaneous adipose tissue of a patient scheduled for visceral surgery after informed consent and ethical approval by the ethics commission of Hannover Medical School. Cell isolation and verification of the donor specific differentiation capacity as well as biochemical pre-differentiation towards vascular SMCs was performed as described recently.¹⁵ Successful pre-differentiation was verified for each culture prior to seeding by evaluating characteristic morphological changes of the cells indicating SMC-phenotypes using light microscopy (Fig. S1). Fibrinogen was isolated from human plasma obtained from donors at the blood donation service at Hannover Medical School after informed consent (Institute for Transfusion Medicine, Hannover Medical School). After pre-differentiation, 3×10^6 cells were suspended in 600 μL of a solution containing 25 mg $\times \text{mL}^{-1}$ cryoprecipitated fibrinogen replenished in human blood serum, 100 $\mu\text{L} \times \text{mL}^{-1}$ M199 10X (Sigma Aldrich, Steinheim, Germany) and 100 U $\times \text{mL}^{-1}$ Aprotinin (Bayer, Lev-

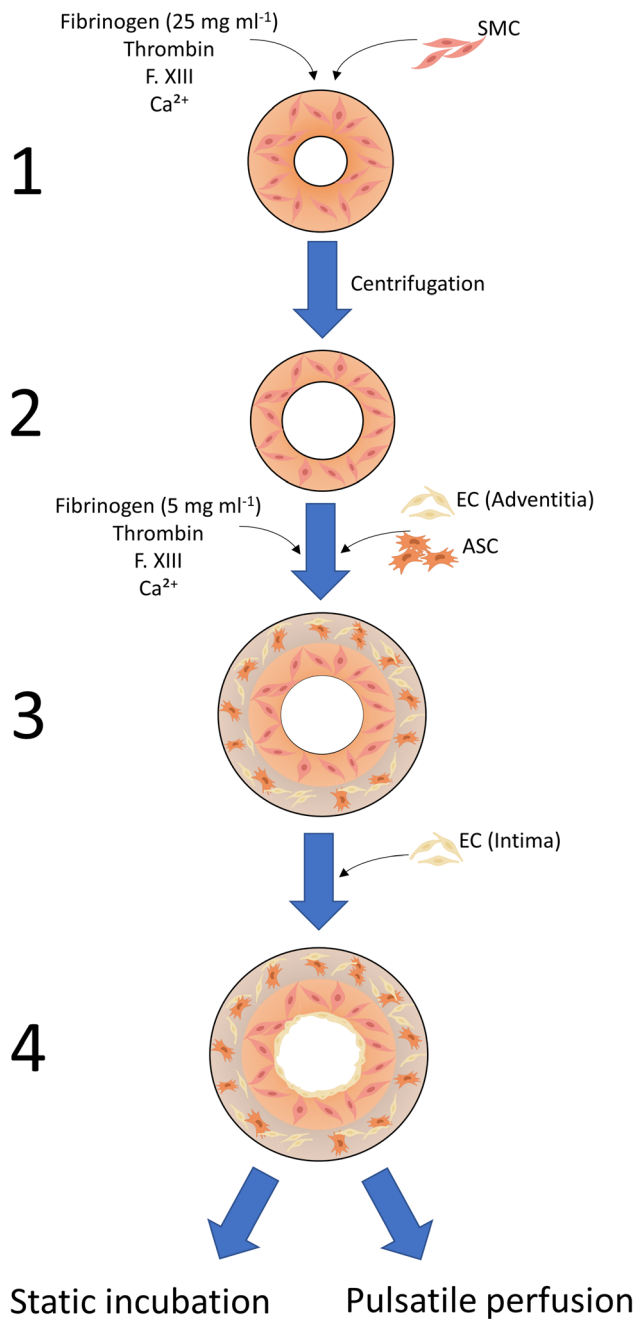


FIGURE 1. Schematic cross sections through the vessel wall showing the steps of the three-layered bioartificial vessel generation. (1) The *tunica media*-equivalent is molded with a high concentration fibrin gel containing smooth muscle cells. (2) The construct is compacted and strengthened in a custom built rotation unit. (3) The *tunica adventitia*-equivalent is molded around it using a low concentration fibrin gel containing endothelial cells and adipose-derived stem cells. (4) Endothelial cells are seeded on the luminal surface to generate the *tunica intima*-equivalent.

erkusen, Germany). pH was adapted by titration of 1 N NaOH. Polymerization was initiated by adding 600 μL of a solution containing $2.5 \text{ U} \times \text{mL}^{-1}$ Thrombin (Vascular Solutions, Mineapolis, USA), $2.5 \text{ U} \times \text{mL}^{-1}$ Factor XIII (CSL Behring, Marburg, Germany) and 40 mM CaCl_2 . The solution was filled in a custom-built cylindrical mold with a diameter of 5 mm.

After 30 min of static polymerization, post-polymerization compaction was performed in a custom-built rotation unit (Department of medical device construction, Hannover Medical School) as described previously.⁸ Here, the *media*-equivalent was centrifugated at $36 \times g$ for 10 min, $145 \times g$ for 10 min and $402 \times g$ for 15 min, which increased mechanical stability and decreased wall thickness (Fig. 1-2).

In the third step (Fig. 1-3), the *media*-equivalent was transferred into a second custom built vascular mold with an outer diameter of 7.75 mm and the *tunica adventitia*-equivalent is molded around the *media*-equivalent. Here, a low-concentration fibrin gel was produced by using a fibrinogen concentration of $5 \text{ mg} \times \text{mL}^{-1}$ with a total volume of 2 mL. 3×10^6 red fluorescent protein expressing human umbilical vein endothelial cells (RFP-HUVECs, Pelo Biotech, Plannegg/Martinsried, Germany) and 3×10^6 ASCs were suspended in the fibrinogen solution and molding was performed as described for step 1.

In the last step, the *tunica intima*-equivalent was generated by luminal seeding with endothelial cells (Fig. 1-4). For this, the fibrin vessels were fixed onto hose-nozzles, a solution of 6×10^6 RFP-HUVECs $\times \text{mL}^{-1}$ suspended in EGM2 (Lonza, Basel, Switzerland) was filled into the lumen of the vessel and the ends were closed using caps. The vessel was incubated in a horizontal position and cells were allowed to attach for a total of 1 h. Every 15 min, the vessel was turned for 90° to ensure complete endothelialization of the luminal circumference.

When seeding was completed, the caps were opened and the vessels were implemented into a custom built bioreactor (Fig. 2b) and exposed to pulsatile perfusion or incubated statically in cell culture tubes (TPP, Trasadingen, Switzerland) (each $n = 3$). For both, perfusion and static incubation, a feeding medium based on M199 containing FGF ($40 \text{ ng} \times \text{mL}^{-1}$), VEGF ($40 \text{ ng} \times \text{mL}^{-1}$), l-ascorbic acid-2-phosphate ($50 \mu\text{g} \times \text{mL}^{-1}$) and aprotinin ($100 \text{ U} \times \text{mL}^{-1}$; all from Sigma) was used.

For the characterization of the biomechanical properties, burst pressure, tensile strength and secant elastic modulus were measured as described previously.²

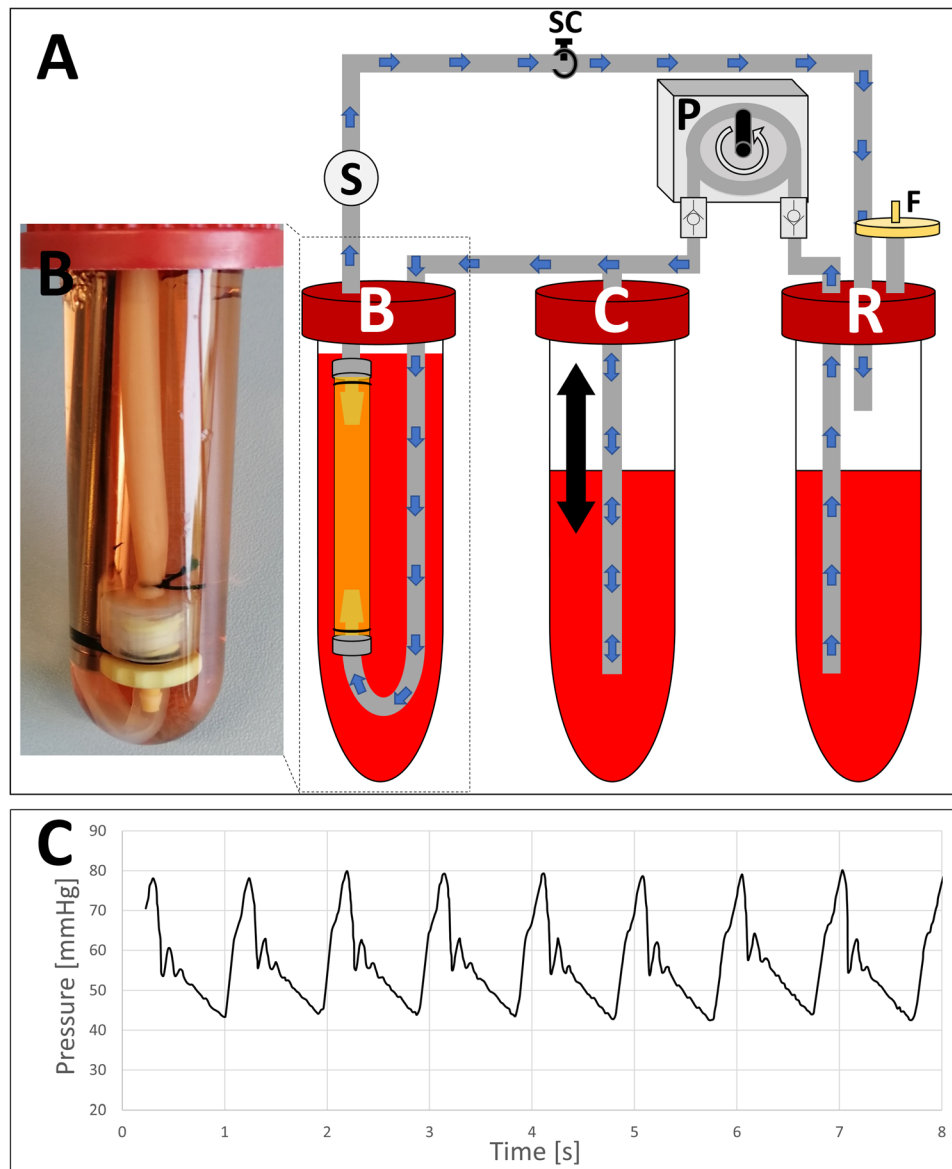


FIGURE 2. Perfusion system setup. **a:** schematic illustration of the pulsatile perfusion system. The bioartificial vessels were placed in a custom built bioreactor (**b**) and pulsatile perfusion was performed using a pulsatile peristaltic pump (**p**) and an air-compliance chamber (**c**). Pressure was adjusted with a screwing clamp (**sc**) and continuously monitored using a pressure sensor (**s**). Gas exchange was facilitated by an open reservoir (**r**) with an air filter (**f**). **b:** photographic close-up showing a bioartificial vessel in the custom built bioreactor. **c:** pressure waveform in an 8 s interval as displayed by the monitoring system.

Pulsatile Perfusion

Pulsatile perfusion was performed in a bioreactor perfusion system (BPS, Fig. 2a) derived and modified from a hemodynamic simulator described in detail elsewhere.⁸

Briefly, a pulsatile peristaltic pump (**P**; Ismatec MCP Standard, Cole Parmer, Wertheim, Germany) was equipped with two check valves to mimic the discontinuous working pattern of the heart and connected to a compliance chamber (**C**) mimicking the ‘Windkessel’ effect of the aorta. The bioreactor (**B**)

containing the bioartificial vessel was placed downstream to that, followed by a pressure sensor (**S**) connected to a monitor system (Datex Ohmeda, Helsinki, Finland) for continuous real-time pressure monitoring. Pressure was adapted using a screwing clamp (**SC**) and gas exchange was facilitated by an open reservoir (**R**). The system was placed in an incubator at 37 °C and 5% CO₂.

The BPS was set to mimic the physiological flow- and pressure environment blood vessels are exposed to in the human body. Prior to starting the perfusion, the vessels were incubated in the bioreactor without flow

TABLE 1. Parameters for pulsatile perfusion obtained in the bioreactor perfusion system in comparison to the physiological range in the human vasculature.

Parameter	Setting	Physiological range
Shear stress (dyn × cm ⁻²)	21.92 ± 1.10	10–70
Pulse frequency (bpm)	60	30–120
Systolic pressure (mmHg)	78.67 ± 1.28	90–120
Diastolic pressure (mmHg)	41.33 ± 0.94	60–80
Pulse pressure (mmHg)	37.33 ± 0.47	30–50
Cyclic stretch (%)	7.55 ± 0.11	5–10

Measured values are given as mean ± standard deviation.

for 12 h to facilitate complete attachment of all cell types. Subsequently, perfusion was started with half of the target flow (30 bpm, 22 mL × min⁻¹) for 10 h to avoid directly exposing luminal RFP-HUVEC to full shear stress. Afterwards, full flow (60 bpm, 44 mL × min⁻¹) was initiated and the vessels were stimulated for 72 h in the BPS under the mechanical conditions shown in Table 1. Cyclic stretch was quantified by obtaining video clips of the segments during perfusion and measuring the maximal (“systolic”) and minimal (“diastolic”) outer vessel diameter as described previously.⁸ Shear stress (τ) was calculated using the following formula:

$$\tau = \frac{4\mu Q}{\pi r^3}$$

with μ \triangleq viscosity of the media, Q \triangleq volume flow and r \triangleq baseline radius of the segment.²⁰

Pulse pressure was defined as follows:

Pulse pressure = systolic pressure – diastolic pressure

Vessel Characterization

After pulsatile perfusion or static incubation, the fibrin vessels were fixed with 4% paraformaldehyde. Vessel dimensions were assessed on cross sections using light-microscopy and layer-specific analysis was performed using fluorescent microscopy (Nikon Eclipse TE300, Düsseldorf, Germany) and the software ImageJ (NIH, Bethesda, USA).

For morphological analysis of the *tunica intima*-equivalent, 5 mm long segments were excised and cut longitudinally to obtain two half-cylinders, which were placed on a microscope slide with the luminal circumference facing towards the objective without additional staining. Thus, only RFP-expressing HUVECs were visualized with fluorescent microscopy for this analysis. Endothelial cell coverage was assessed by

marking the cell-covered luminal area of 10 fields in 10-fold primary magnification and using the following formula:

$$\text{EC Coverage (\%)} = \frac{\text{Covered Area}}{\text{Total Area}} * 100\%$$

Cell orientation was analyzed by marking the main axis of each cell in 5 fields in 20-fold primary magnification for each vessel and comparing them to the longitudinal axis of the vessel, which was defined as 0°.

Evaluation of the *tunica media* was performed on 6 μ m thick cryosections, which were stained for SMC-specific cell markers. Therefore, sections were fixed with 4% paraformaldehyde, permeabilized using 0.1% Triton-X-100 and blocked with PBS containing 10% fetal calf serum, 0.1% bovine serum albumin and 0.05% Tween-20 (all from Sigma-Aldrich). Immunostaining was performed using the antibodies ‘Mouse alpha smooth muscle actin’ (1:100; DM001, Acris Antibodies, Herford, Germany) and ‘rabbit calponin’ (1:100; ab46794; Abcam, Cambridge, UK). Alexa Fluor 555 coupled anti rabbit IgG and Alexa Fluor 488 coupled anti mouse IgG were used as secondary antibodies. To counterstain nuclei, sections were mounted with medium containing 4,6-diamidino-2-phenylindole (DAPI, Carl Roth GmbH, Karlsruhe, Germany).

The *tunica adventitia*-equivalent was assessed on 5 mm long segments, which were excised, opened longitudinally and placed on a microscope slide with the outer circumference facing towards the objective. Vascular tube formation was quantified using the software ‘AngioTool’³⁵ on 5 fields in 10-fold primary magnification for each vessel. Additionally, 12 μ m thick longitudinal cryosections were obtained and nuclei were again counterstained with DAPI. To confirm presence of a lumen in the microvascular structures, cross-sections of the adventitia were analyzed by laser scanning fluorescent microscopy using the ‘Olympus FluoView 1000’ confocal laser scanning microscope (Olympus Europe, Hamburg, Germany) with a 555 nm excitation wave length and an emission wave length ranging from 564 to 620 nm.

Statistics

Statistical analyses were performed by using the software ‘Graphpad Prism 6.04’ (Graphpad software, San Diego, USA). Normal distribution was tested with D’Agostino and Pearsons omnibus normality test. Unpaired Student’s *t*-test was used to compare two groups. Differences were considered significant at $p < 0.05$.

RESULTS

Technical Aspects

The bioreactor system developed in this study was characterized with respect to its accuracy for *in vitro* simulation of the physiological mechanical environment that blood vessels are exposed to in the human body. The mechanical conditions obtained in the bioreactor perfusion system are shown in Table 1 and Fig. 2c. While shear stress, pulse pressure, pulse frequency and cyclic distension were well within the physiological range of the human vasculature, slightly lower systolic and diastolic pressures were applied due to the relative higher compliance of fibrin vessels compared to native arteries as indicated by the secant elastic modulus. The pressure-waveform shows a di-crotic morphology indicating accurate simulation of the physiological arterial pressure curve in small diameter vessels.¹⁰

Overall Vessel Wall Architecture

The manufacturing process resulted in stable and homogeneous fibrin vessels with a burst pressure of 191.78 ± 24.64 mmHg, tensile strength of $20.11 \text{ kPa} \pm 4.90 \text{ kPa}$ with a secant elastic modulus of $3.74 \text{ kPa} \times \text{mm}^{-1} \pm 0.56 \text{ kPa} \times \text{mm}^{-1}$ and an initial wall thickness of 3.05 mm (Fig. 3a). Both static and dynamic incubation reduced the thickness of the vessel wall after 72 h, which was slightly more pronounced with

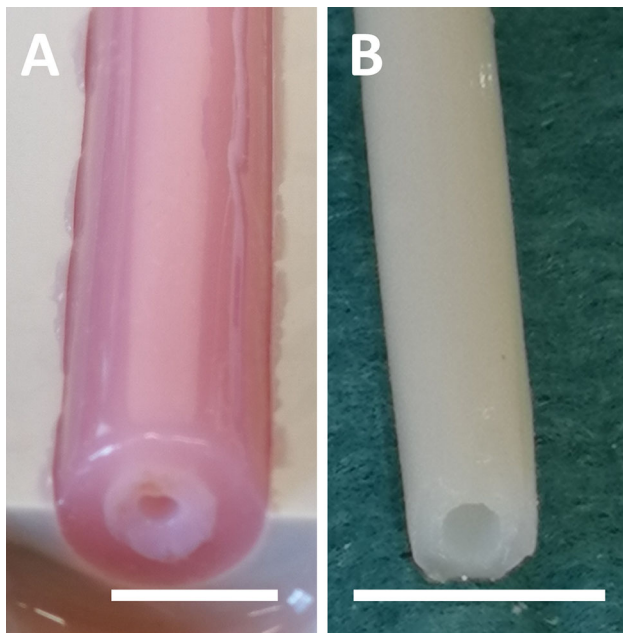


FIGURE 3. Macroscopic morphology of the three-layered bioartificial vessel in the opened vascular mold after molding of the *tunica adventitia*-equivalent (a) and after pulsatile perfusion for 72h (b). Scale bar = 5 mm.

static incubation (75.3% vs 72.2%, Table 2). This can also be appreciated qualitatively in Fig. 3. Moreover, the reduction of the luminal diameter was more pronounced in the statically incubated group.

To evaluate the overall structure of the bioartificial vessel wall, cross sections were stained and analyzed by fluorescence microscopy (Fig. 4). In both groups, the vessel was built up by three clearly distinct layers seeded with the respective layer-specific cell types. On the luminal surface, a closed endothelial cell layer formed by RFP-HUVEC was observed. Within the fibrin matrix, two additional layers were present: The middle one contained α SMA-positive cells and the outer layer was interwoven with RFP-HUVEC in a scattered distribution. Equal cellularity was observed in both groups. Thus, the manufacturing technique was successful in generating a stable three-layered vessel construct. Each layer was further characterized after incubation with or without mechanical stimulation.

Effect of Pulsatile Perfusion

Pulsatile perfusion influenced the morphology of each layer. At first, the inner layer was examined under fluorescence microscopy of the luminal surface of the bioartificial vessels cultivated under static and dynamic conditions (Fig. 5). Cell coverage was equal for both groups with $86.8\% \pm 1.56\%$ in the static group and $86.7\% \pm 0.78\%$ in the mechanically stimulated group ($p = 0.91$). However, endothelial cells showed a longitudinal alignment parallel to the vessel axis and flow direction when exposed to pulsatile perfusion (Figs. 5a and 5b). Quantitative analysis of the cell orientation confirmed this orientation of the luminal HUVEC monolayers by showing a gaussian distribution with the highest number of cells in the range of -5° to $+5^\circ$ relative to the vessel axis (Figs. 5c and 5d). In contrast to that, random orientation was observed in the static control group. In both groups, no vascular tube formation was present on the luminal surface. Additionally, no evidence for unintended SMC-cellularization of the *intima*-layer was found (Fig. S2).

In the middle layer, SMC alignment and marker expression were analyzed immunohistochemically on cross sections of the vessel wall (Fig. 6). Cells in statically and dynamically incubated vessels showed co-expression of the early marker α SMA and the more specific SMC marker protein Calponin confirming successful myogenic differentiation from ASC. SMC in the static control showed a random cell orientation. In contrast, as shown recently,⁸ pulsatile perfusion resulted in a circular SMC alignment perpendicular to the vessel axis similar to the *tunica media* of natural arterial vessels.

TABLE 2. Vessel dimensions measured on light microscopy images of cross sections after 72 h of static or pulsatile dynamic cultivation.

	Static incubation	Pulsatile perfusion	<i>p</i> value	Natural carotid artery ^{30b}
Luminal diameter (μm)	1363 \pm 17	1504 \pm 27	< 0.001	
Total wall thickness (μm)	754 \pm 65	847 \pm 63	0.22	\approx 1130
Media thickness (μm) ^a	437 \pm 53	477 \pm 29	0.25	\approx 630
(relative media thickness (%))	(53.7 \pm 2.5)	(55.3 \pm 2.5)		(\approx 55.8)
Adventitia thickness (μm) ^a	364 \pm 14	379 \pm 43	0.42	\approx 500
(Relative adventitia thickness (%))	(46.3 \pm 2.7)	(44.7 \pm 2.5)		(\approx 44.2)
Outer diameter (μm)	1976 \pm 78	2351 \pm 23	< 0.01	

Values are given as mean \pm standard deviation.

^aTo allow comparison among vessels with different total wall thickness, the relative media and adventitia thickness in relation to the total wall thickness was calculated and is given in (%).

^bWall thickness of the carotid artery of healthy individuals with low cardiovascular risk described by Skilton *et al.*³⁰ serve as comparison.

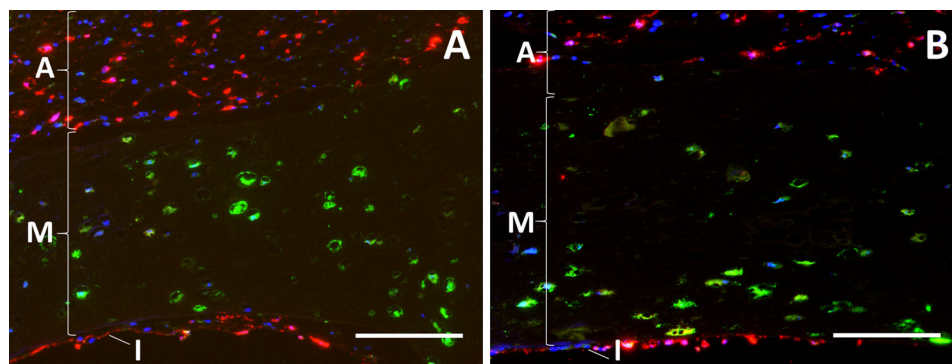


FIGURE 4. Overall vessel wall morphology. The three-layered wall of the bioartificial vessels after 72 h of static incubation (a) or pulsatile perfusion (b) is shown in cross sections of the vessel wall. RFP-HUVEC (red) indicate the *tunica intima*-equivalent on the luminal surface (l) and capillary tubes of the *tunica adventitia*-equivalent in the abluminal part of the vessel wall (a). Smooth muscle cells of the *tunica media*-equivalent (m) and adipose-derived stem cells in the bioartificial *tunica adventitia* are visualized by immunofluorescence staining of α smooth muscle actin (green). Nuclei were counterstained using 4,6-diamidino-2-phenylindole (DAPI). Scale bar = 100 μm , RFP-HUVEC Red-fluorescent protein expressing human umbilical vein endothelial cells.

Microscopic investigation of the abluminal surface of the bioartificial vessels demonstrated a complex network of tubular structures under static conditions with a random orientation (Fig. 7a). Interestingly, pulsatile perfusion induced an oriented structure of this capillary network. Similar to the luminal endothelial cells, also the vascular tubes aligned strictly parallel to the longitudinal vessel axis after pulsatile perfusion (Fig. 7b). Network analysis by ‘AngioTool’ software revealed that in these longitudinal tubes, branching existed exclusively in form of bifurcations (Fig. 7d). In contrast, randomly orientated tubes on the abluminal surface of the statically incubated vessels showed a branching pattern with bi-, tri- and quadri-furcations (Fig. 7c). ‘Angio-Tool’ analysis also revealed a higher number of junctions per microscopic field in the statically incubated group (138.93 \pm 16.88 vs. 78.13 \pm 3.43, $p < 0.01$; Fig. 8). Additionally, tube density was slightly but significantly higher compared

to the pulsatile perfusion group whereas the total vessel length did not change (Fig. 8).

The morphology of the vascular networks was further assessed on longitudinal cryosections (Figs. 7e and 7f) confirming that the respective tube orientation was present throughout all zones of the outer layer. Moreover, it was observed that under dynamic conditions tubes consisted of several aligned endothelial cells, whereas under static conditions no similar structures were observed. The arrow in Fig. 7f marks an exemplary longitudinally oriented tube that consists of at least four different HUVECs as indicated by counterstaining of the nuclei.

Finally, it was evaluated whether the longitudinal tubes contained a lumen. Laser scanning microscopy clearly showed a lumen in the cross section of a microvascular tube and thus, confirmed it as a capillary-like structure (Fig. 7g).

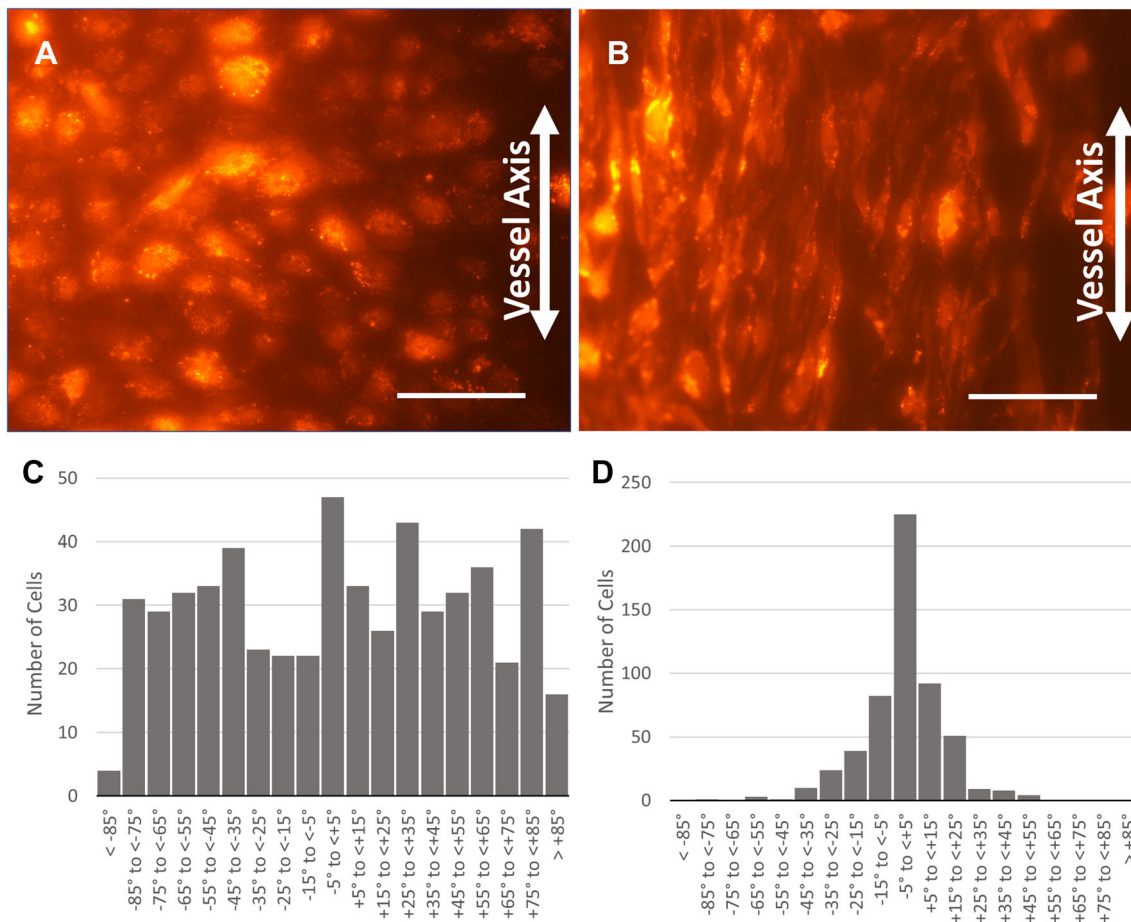


FIGURE 5. Evaluation of the *tunica intima*-equivalent. Endothelial coverage by RFP-HUVEC (red) was assessed on fluorescence microscopy images of the luminal surface of the bioartificial vessels after 72 h static incubation (a) or pulsatile perfusion (b). Cell alignment was quantified on 5 microscopic fields in 20-fold primary magnification for each vessel. Frequency distribution of the main axis of the cells is shown as deviation from the longitudinal vessel axis, which was defined as 0° (c static incubation: total cell number: 560; d pulsatile perfusion, total cell number: 549). Scale bar = 100 μ m, RFP-HUVEC Red-fluorescent protein expressing human umbilical vein endothelial cells.

DISCUSSION

In this study, we developed a tissue engineering technique for the generation of three layered fibrin-based bioartificial blood vessels by combining a stepwise molding technique and physiological mechanical stimulation. The insights resulting from this *in vitro* proof-of-concept study can be summarized as follows: (i) Fibrin-based matrices of different concentrations and mechanical properties can be combined to a three layered bioartificial vessel wall facilitating seeding with the cell types relevant for *in vitro* vascular tissue engineering. (ii) All three layers of natural blood vessels were emulated within the physiologically structured bioartificial vessel wall after short-term culture of 72 h. (iii) Physiological mechanical stimulation in a sophisticated BPS is of pivotal importance to facilitate proper cell alignment in all three layers of the vascular wall. (iv) In this context, it was shown for the first time that

biomechanical stimulation induced a parallel alignment of hollow capillary structures in an artificial *tunica adventitia*-equivalent.

Stepwise Fibrinogen Molding Technique

The need to resemble the physiological architecture of the vascular wall in bioartificial vessels has been recognized for a long time, and first attempts to generate three-layered cellularized vascular constructs have been made in different fields of tissue engineering. A very popular approach is the use of 3D-bioprinting, which allows for the generation of complex three-dimensional constructs.⁷ One example of a bioprinting approach targeting the vascular wall was provided by Schöneberg *et al.*, who generated three-layered vascular channels in a fibrin/collagen matrix with subsequent fluid perfusion.²⁸ However, the maximal fibrinogen concentration applicable for the bioprinting

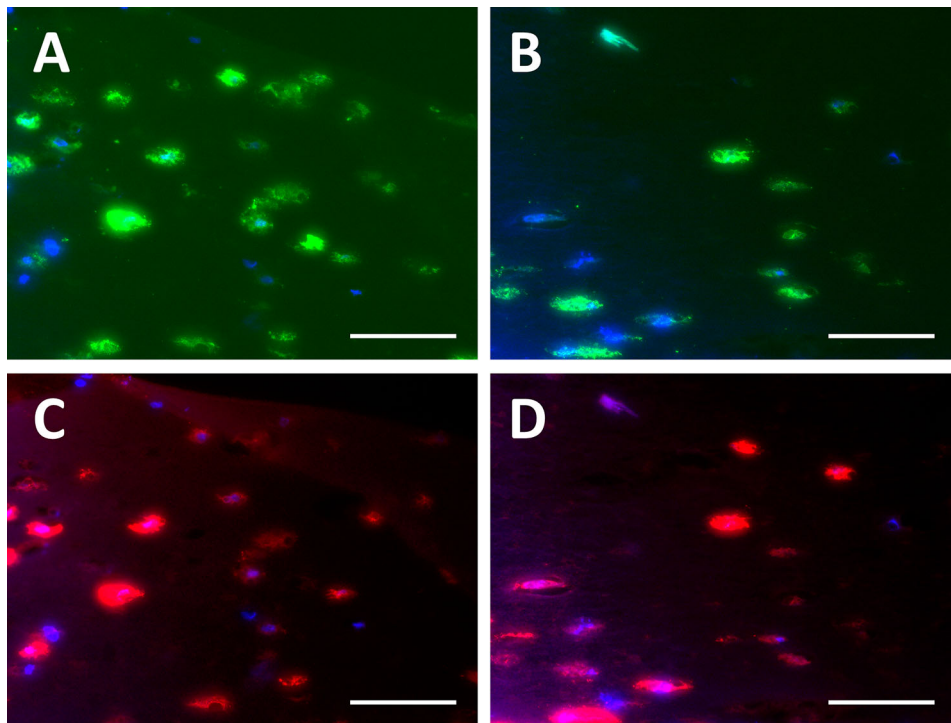


FIGURE 6. Evaluation of the *tunica media*-equivalent. Cross sections of the vessel wall (same orientation as in Fig. 4) after 72 h static incubation (a, c) or pulsatile perfusion (b, d) were stained for the smooth muscle cell marker proteins α smooth muscle actin (a, b; green) and calponin (c, d, red). Nuclei were counterstained using 4,6-diamidino-2-phenylindole (DAPI). Scale bar = 100 μm .

technique was limited to only 2.5% and the generated constructs were not suitable for regenerative approaches including *in vitro* mechanical conditioning. Opposed to that, mechanical stability of the fibrin matrix generated by our molding technique with subsequent centrifugation was sufficient to generate self-supporting vessels suitable for mechanical stimulation under pulsatile pressure conditions.

As an alternative technique, Iwasaki *et al.* generated mechanically robust three-layered bioartificial vessels using cellularized polyglycolic acid (PGA)- and polygalactone-sheets and subsequent pulsatile perfusion in a BPS.¹² While this study underlines the importance of mechanical stimulation for generating the physiological morphology of the vascular wall, the applicability of these bioartificial vessels for regenerative approaches is limited due to the use of bovine cells and biodegradable scaffolds, which potentially produce cytotoxic degradation products.²⁹ In our study, we used HUVECs and human ASCs as cell sources. ASCs are known to be an easily accessible and thus, potentially autologous cell source for vascular tissue engineering approaches³ and respond well to both biochemical and biomechanical differentiation factors.⁸ Moreover, fibrinogen can be easily precipitated in large amounts from peripheral blood making fibrin

an ideal biological matrix material for bioartificial vessels. It allows seeding of multiple cell types²⁹ and its degradation products are not toxic. Its high biocompatibility has been studied and proven extensively since fibrin glue is used frequently as a sealant for adjuvant hemostasis in cardiovascular surgery for many years.²⁶ On the other hand, the mechanical stability of fibrin based vascular grafts is considerably lower than that of natural vessels or synthetic polymers. The burst pressure and tensile strength observed in this study was sufficient for *in vitro* pulsatile stimulation, but higher safety margins have to be achieved when clinical application is targeted in the future.

The decrease in wall thickness of cellularized fibrin constructs during the culture period is a known phenomenon,⁸ which appears to be even more pronounced in this study due to the low fibrinogen concentration of the *tunica adventitia*. Comparison of the relative media- and adventitia-thickness of the graft with physiological values of the carotid artery of healthy individuals with low cardiovascular risk³⁰ shows similarity for both groups with a lower absolute wall thickness (Table 2).

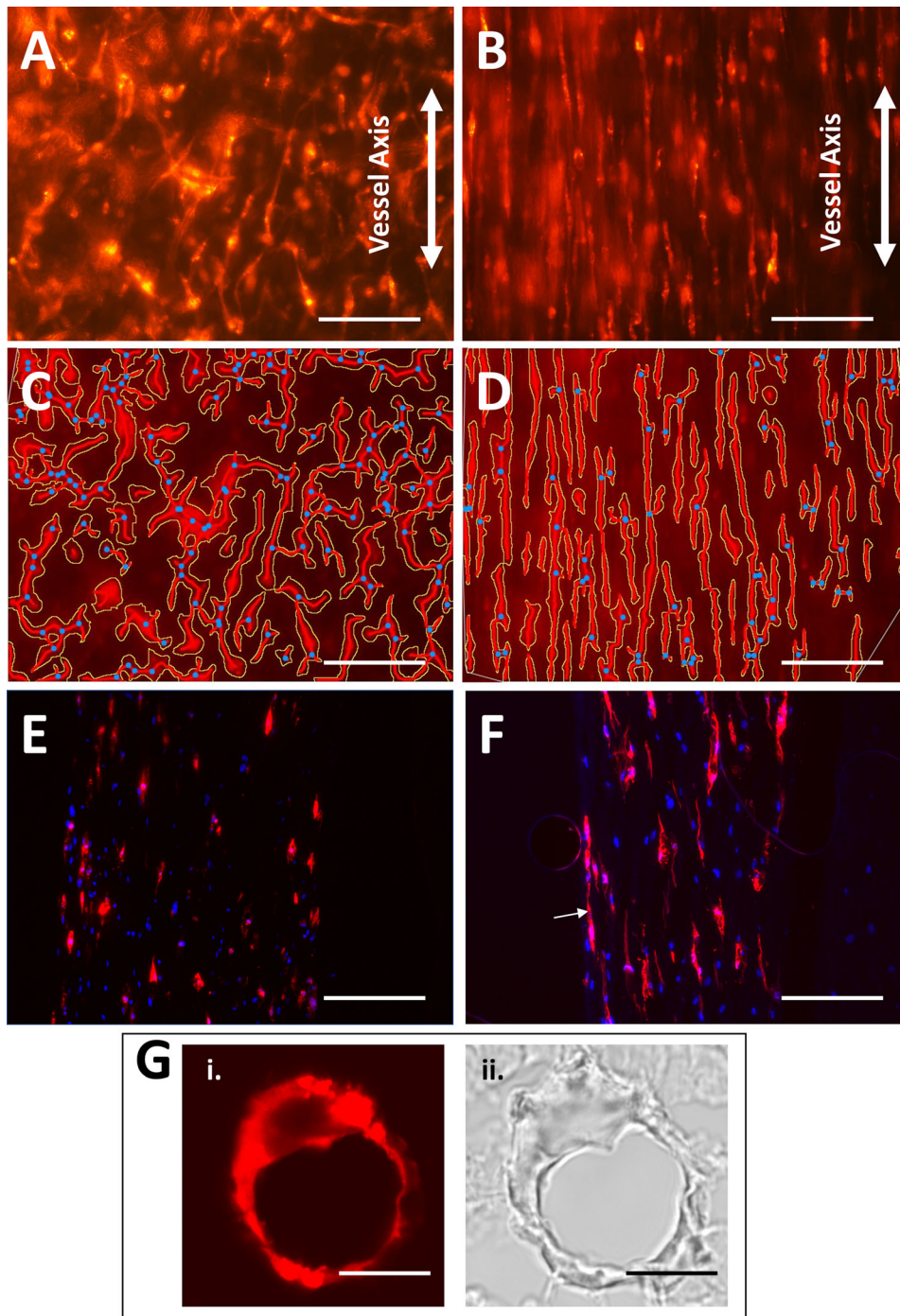


FIGURE 7. Evaluation of the *tunica adventitia*-equivalent. Tube formation by RFP-HUVEC was assessed on fluorescence microscopy images of the abluminal surface of the bioartificial vessels after 72 h static incubation (a) or pulsatile perfusion (b). (c) and (d) show images a and b after analysis by the 'Angiotool'-software, which was used for quantification of the vascular network properties. (e) and (f) show cryosections of the vessel wall parallel to the longitudinal vessel axis. Nuclei were counterstained with DAPI. The arrow indicates an exemplary tube formed by at least 4 cells. Scale bar = 100 μm , RFP-HUVEC Red-fluorescent protein expressing human umbilical vein endothelial cells. (g) Shows a laser-scanning-microscopic image of a cross section of a microvascular tube indicating the presence of an open lumen. (i) Laser scanning image with excitation wave length of 555 nm and emission wave length ranging from 568 to 620 nm (ii) Respective bright field image, Scale bar = 10 μm .

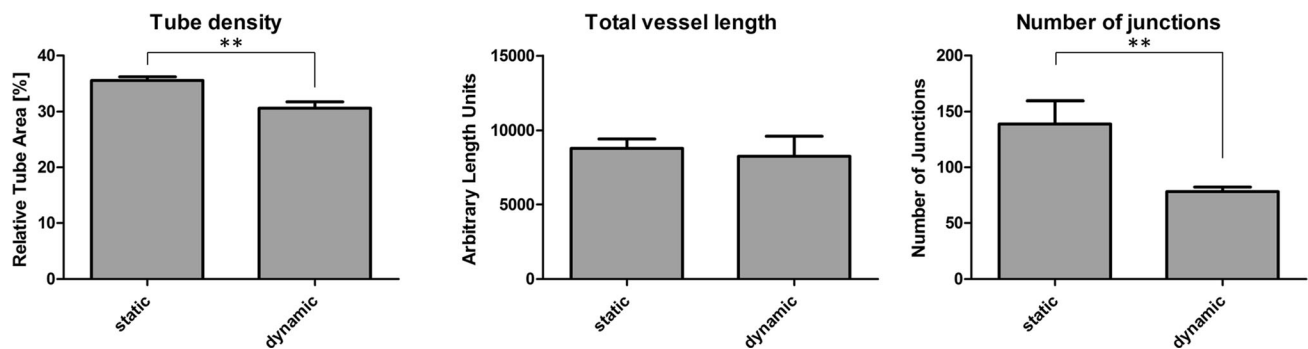


FIGURE 8. Quantitative comparison of the microvascular network parameters. Tube networks of the outer layer of independent manufactured vessels ($n = 3$ for each group) were analyzed by 'Angiotool' software. For the indicated tube parameters, means \pm SEM of 5 images per vessel are shown. Tube density was defined as the fraction of each field covered by microvascular structures (= relative tube area), total vessel length is the sum of the lengths of all vessels within one analysis field and number of junctions represents the total number of branching points per analysis field $**p < 0.01$ by unpaired Student's *t*-test.

Generation and Mechanical Stimulation of the Tunica Intima-Equivalent

A confluent endothelial cell layer in the *tunica intima* is of pivotal importance for hemocompatibility of bioartificial vessels.²¹ In this study, the percentage area covered with endothelial cells was high in both, the static and biomechanically stimulated three-layered vessels. This shows that endothelial cell attachment was sufficient to withstand physiological shear rates and stretch amplitudes. This strong cell attachment to the fibrin matrix, that has also been shown by Isenberg *et al.*¹¹ again underlines suitability of fibrin as a matrix material in vascular tissue engineering.

Mechanical stimulation in the BPS induced endothelial cell elongation and alignment parallel to the vessel axis, which resembles the physiological alignment in natural blood vessels. On the contrary, no elongation or directed alignment was observed on the luminal surface of statically incubated three-layered vessels. It long has been known that endothelial cells respond to shear stress with a variety of effects including alignment parallel to flow.²⁴ Moreover, cyclic stretch¹³ and potentially also luminal pressure¹⁹ have been shown to influence endothelial cell alignment and connectivity. Since the BPS used here exerted flow, stretch and pressure on the luminal surface, most likely all three mechanical stimuli influenced endothelial cell alignment synergistically and thus induced the strict longitudinal cell orientation in this *tunica intima*-like layer.

Generation and Mechanical Stimulation of the Tunica Media-Equivalent

Biochemical differentiation of ASC to multiple mesenchymal cell types has been studied extensively in the past.³⁶ Additionally, the response of ASCs to

mechanical differentiation factors is well known.⁸ This analysis also revealed that differentiation capacity of ASC is donor dependent and thus requires sound characterization as described previously.¹⁵ This also required selection of a suitable donor for SMC differentiation in this study. Here, the relatively short mechanical stimulation time of 72 h was sufficient to induce circular orientation of the SMCs around the vessel lumen resembling the natural arrangement of the *tunica media* while random orientation of the cells was observed in the statically incubated vessels. However, much longer culture times are usually required to facilitate extracellular matrix production by seeded cells.⁸ Circular alignment is of pivotal importance to accomplish contraction of the vessel diameter, which represents the main function of the *tunica media* in natural blood vessels. The suitability of mechanically stimulated SMC to induce contractility in fibrin-based grafts is described extensively elsewhere.⁸ Moreover, SMCs of the perfused vessels showed a spindle-like morphology, which is characteristic for the desired contractile phenotype of SMCs.²³

Expression of the SMC marker proteins alpha smooth muscle actin (α SMA) and Calponin was assessed qualitatively by immunohistochemical staining. Despite deprivation from biochemical growth factors during the cultivation period both, the static and dynamic group were stained positive for these marker proteins. This confirms successful biochemical differentiation towards SMC lineage prior to cell seeding without markable de-differentiation during culture in the bioartificial vessels.

Generation and Mechanical Stimulation of the Tunica Adventitia-Equivalent

To generate a vascular network in the *tunica adventitia*, RFP-HUVECs were co-seeded with ASCs

in a low concentration fibrin matrix and extensive tube formation was observed in both groups. We have previously shown that fibrin gels with a fibrinogen concentration of $5 \text{ mg} \times \text{mL}^{-1}$ are suitable for vascular tube formation by cell self-assembly but provide only low mechanical strength.³⁴ In the three-layered bioengineered vessel, the compacted and highly concentrated fibrin matrix of the *tunica media* provided sufficient mechanical strength for pulsatile perfusion. This is in consistence with natural arteries, in which the *tunica media* contributes most to mechanical stability. Thus, the *tunica adventitia*-equivalent was not directly exposed to the intraluminal pressure facilitating the use of a low concentration fibrin matrix. The co-culture technique with ASCs has been shown to improve capillary tube formation in fibrin matrices by us and others.^{9,34} As potential mechanisms for the induction and stabilization of tube formation by ASC, Rohringer *et al.* showed induction of genes relevant for tube formation in HUVEC in co-culture with ASC.²⁵ Furthermore, we previously described that ASC take on a pericyte-like function in co-cultures with endothelial cells and thus, stabilize the vascular network.¹⁶

In contrast to this study, the vast majority of tissue engineering approaches targeting the *tunica adventitia* was focused on integrating fibroblasts producing extracellular matrix proteins like collagen.^{12,18,28,32} Though this is certainly an important feature, it should be noted that the natural *adventitia* in human blood vessels is far more complex than a simple collagen layer as it includes multiple structures and has a variety of functions crucial for vessel biology.³¹ A proper nutrient and oxygen supply facilitated by the vascular capillary structures of the *tunica adventitia* is essential for the entire vessel wall. Thus, vascularization of the *tunica adventitia* should be considered a key feature in vascular tissue engineering approaches as well. In this context, ASC represent suitable stromal supporting cells for *in vitro* vascular tissue engineering because they facilitate tube formation and can be differentiated to SMC for the use in the *media*-equivalent as well.

Specifically for fibrin-based bioartificial vessels, limited cellularization in deeper layers of the vessel wall due to insufficient vascularization and thus, nutrition, is a long known limitation.¹

One of the very few tissue engineering approaches targeting the *vasa vasorum* of the *adventitia* was published by Guillemette *et al.*⁶ They showed that vascularization of *adventitia*-equivalents generated by cell self-assembly facilitated graft integration and perfusion after subcutaneous implantation into mice. Importantly, only minimal *in vivo* vascularization was observed in *adventitia* equivalents that were not pre-vascularized *in vitro*. This again underlines the importance of generating a properly vascularized

adventitial tissue as presented here in form of the three-layered vessel with regards to regenerative approaches.

Considering these findings, generating three-layered bioartificial vessels with a pre-vascularized *adventitia* is a promising strategy to overcome the limitation concerning cellularization of thicker vessel walls in fibrin-based bioartificial vessels. In our study, complete cellularization of the full thickness of the vessel wall was observed in both the statically and the dynamically cultured three-layered vessels indicating sufficient nutrient or oxygen supply throughout the vessel wall.

Although capillary-like tube formation was observed in both groups, the overall structure of the tubes differed distinctively. While a random tubular network with multiple branching points was observed in the static group, the tubes in the *adventitia* of the dynamic group were aligned strictly parallel to the vessel axis with fewer branching points. Until now, only very little is known about the impact of mechanical stretch on vascular tube formation. Russo *et al.* describe an amplitude dependent increase or decrease in angiogenesis by endothelial cells subjected to stretch in a 2-dimensional vacuum stretching system without any noticeable influence on tube alignment or direction.²⁷ When comparing these results to our findings, it should be noted that endothelial cells in the three-layered vessel are seeded into a 3-dimensional biological matrix and exposed to a complex multiaxial stretch induced by pulsatile perfusion instead of a 2-dimensional silicon membrane facilitating only uniaxial stretch.

The longitudinal alignment of vascular tubes parallel to the vessel axis with bifurcating branches resembles the alignment of *vasa vasorum* capillaries in the *adventitia* of natural vessels, that has been studied and described extensively by Lametschwandtner *et al.* on human saphenous veins.¹⁴ To our knowledge, vascular tube alignment induced by mechanical stimulation has not been reported yet and will be further investigated in subsequent studies targeting this phenomenon specifically.

While this study focused on the emulation of the microvascular components of the *adventitia*, using longer culture times to facilitate extracellular matrix construction by ASC or adding collagen producing cells such as fibroblasts could potentially facilitate an even more accurate emulation of this complex layer.

Moreover, studies are needed to investigate the long term impact of cellularization on mechanical and functional properties of three-layered grafts. Additionally, the generation of the inner and outer elastic membrane, which are characteristic for larger arteries, was not targeted in this study and represents another goal to potentially facilitate even more accu-

rate emulation of the natural vessel wall architecture in bioartificial vascular grafts.

SUPPLEMENTARY INFORMATION

The online version of this article (<https://doi.org/10.1007/s10439-021-02728-9>) contains supplementary material, which is available to authorized users.

ACKNOWLEDGMENTS

The work was funded by the German Society for Implant Research and Development (funding title: “Vascularization of bioartificial implants 2017–2020”).

REFERENCES

- ¹Aper, T., O. E. Teebken, G. Steinhoff, and A. Haverich. Use of a fibrin preparation in the engineering of a vascular graft model. *Eur. J. Vasc. Endovasc Surg.* 28(3):296–302, 2004.
- ²Aper, T., M. Wilhelmi, C. Gebhardt, K. Hoeffler, N. Benecke, A. Hilfiker, *et al.* Novel method for the generation of tissue-engineered vascular grafts based on a highly compacted fibrin matrix. *Acta Biomater.* 29:21–32, 2016.
- ³Bajpai, V. K., and S. T. Andreadis. Stem cell sources for vascular tissue engineering and regeneration. *Tissue Eng. Part B Rev.* 18(5):405–425, 2012.
- ⁴Enomoto, S., M. Sumi, K. Kajimoto, Y. Nakazawa, R. Takahashi, C. Takabayashi, *et al.* Long-term patency of small-diameter vascular graft made from fibroin, a silk-based biodegradable material. *J. Vasc. Surg.* 51(1):155–164, 2010.
- ⁵GBD. Mortality and causes of death collaborators. Global, regional, and national age-sex specific all-cause and cause-specific mortality for 240 causes of death, 1990–2013: a systematic analysis for the Global Burden of Disease Study 2013. *Lancet.* 385(9963):117–171, 2013.
- ⁶Guillemette, M. D., R. Gauvin, C. Perron, R. Labbé, L. Germain, and F. A. Auger. Tissue-engineered vascular adventitia with vasa vasorum improves graft integration and vascularization through inosulation. *Tissue Eng Part A.* 16(8):2617–2626, 2010.
- ⁷Hann, S. Y., H. Cui, T. Esworthy, S. Miao, X. Zhou, S. Lee, *et al.* Recent advances in 3D printing: vascular network for tissue and organ regeneration. *Transl Res.* 09(211):46–63, 2019.
- ⁸Helms, F., S. Lau, M. Klingenberg, T. Aper, A. Haverich, M. Wilhelmi, *et al.* complete myogenic differentiation of adipogenic stem cells requires both biochemical and mechanical stimulation. *Ann Biomed Eng.* 48:913–926, 2019.
- ⁹Holthoner, W., K. Hohenegger, A. Husa, S. Muehleder, A. Meinl, A. Peterbauer-Scherb, *et al.* Adipose-derived stem cells induce vascular tube formation of outgrowth endothelial cells in a fibrin matrix. *J Tissue Eng Regen Med.* 9(2):127–136, 2015.
- ¹⁰Huang, C., D. Chambers, and G. Matthews. Arterial Pressure Waveforms. In: *Basic Physiology for Anaesthetists* 2nd, edited by C. Huang, D. Chambers, and G. Matthews. Cambridge: Cambridge University Press, 2019, pp. 155–157.
- ¹¹Isenberg, B. C., C. Williams, and R. T. Tranquillo. Endothelialization and flow conditioning of fibrin-based media-equivalents. *Ann Biomed Eng.* 34(6):971–985, 2006.
- ¹²Iwasaki, K., K. Kojima, S. Kodama, A. C. Paz, M. Chambers, M. Umez, *et al.* Bioengineered three-layered robust and elastic artery using hemodynamically-equivalent pulsatile bioreactor. *Circulation.* 118(14):52, 2008.
- ¹³Jufri, N. F., A. Mohamedali, A. Avolio, and M. S. Baker. Mechanical stretch: physiological and pathological implications for human vascular endothelial cells. *Vasc. Cell.* 7:8, 2015.
- ¹⁴Lametschwandtner, A., B. Minnich, D. Kachlik, M. Setina, and J. Stingl. Three-dimensional arrangement of the vasa vasorum in explanted segments of the aged human great saphenous vein: scanning electron microscopy and three-dimensional morphometry of vascular corrosion casts. *Anat. Rec. A Discov. Mol. Cell Evol. Biol.* 281(2):1372–1382, 2004.
- ¹⁵Lau, S., M. Klingenberg, A. Mrugalla, F. Helms, D. Sedding, A. Haverich, *et al.* Biochemical myogenic differentiation of adipogenic stem cells is donor dependent and requires sound characterization. *Tissue Eng. Part A.* 25(13–14):936–948, 2019.
- ¹⁶Lau, S., C. Schrimpf, M. Klingenberg, F. Helfritz, T. Aper, A. Haverich, *et al.* Evaluation of autologous tissue sources for the isolation of endothelial cells and adipose tissue-derived mesenchymal stem cells to pre-vascularize tissue-engineered vascular grafts. *BioNanoMaterials.* 16(4):309–321, 2015.
- ¹⁷Lawson, J. H., M. H. Glickman, M. Ilzecki, T. Jakimowicz, A. Jaroszynski, E. K. Peden, *et al.* Bioengineered human acellular vessels for dialysis access in patients with end-stage renal disease: two phase 2 single-arm trials. *Lancet.* 387(10032):2026–2034, 2016.
- ¹⁸L’Heureux, N., S. Pâquet, R. Labbé, L. Germain, and F. A. Auger. A completely biological tissue-engineered human blood vessel. *FASEB J.* 12(1):47–56, 1998.
- ¹⁹Müller-Marschhausen, K., J. Waschke, and D. Drenckhahn. Physiological hydrostatic pressure protects endothelial monolayer integrity. *Am. J. Physiol. Cell Physiol.* 294(1):324, 2008.
- ²⁰Papaioannou, T. G., and C. Stefanadis. Vascular wall shear stress: basic principles and methods. *Hellenic J Cardiol.* 46(1):9–15, 2005.
- ²¹Pawlowski, K. J., S. E. Rittgers, S. P. Schmidt, and G. L. Bowlin. Endothelial cell seeding of polymeric vascular grafts. *Front. Biosci.* 9:1412–1421, 2004.
- ²²Pennings, I., E. E. van Haften, T. Jungst, J. A. Bulsink, A. J. W. P. Rosenberg, J. Groll, *et al.* Layer-specific cell differentiation in bi-layered vascular grafts under flow perfusion. *Biofabrication.* 12(1):015009, 2019.
- ²³Rensen, S. S., P. A. Doevendans, and G. J. van Eys. Regulation and characteristics of vascular smooth muscle cell phenotypic diversity. *Neth Heart J.* 15(3):100–108, 2007.
- ²⁴Resnick, N., H. Yahav, A. Shay-Salit, M. Shushy, S. Schubert, L. C. M. Zilberman, *et al.* Fluid shear stress and the vascular endothelium: for better and for worse. *Prog. Biophys. Mol. Biol.* 81(3):177–199, 2003.

- ²⁵Rohringer, S., P. Hofbauer, K. H. Schneider, A. Husa, G. Feichtinger, A. Peterbauer-Scherb, *et al.* Mechanisms of vasculogenesis in 3D fibrin matrices mediated by the interaction of adipose-derived stem cells and endothelial cells. *Angiogenesis*. 17(4):921–933, 2014.
- ²⁶Rousou, J. A. Use of fibrin sealants in cardiovascular surgery: a systematic review. *J. Card. Surg.* 28(3):238–247, 2013.
- ²⁷Russo, T. A., D. Stoll, H. B. Nader, and J. L. Dreyfuss. Mechanical stretch implications for vascular endothelial cells: altered extracellular matrix synthesis and remodeling in pathological conditions. *Life Sci.* 213:214–225, 2018.
- ²⁸Schöneberg, J., F. De Lorenzi, B. Theek, A. Blaeser, D. Rommel, A. J. C. Kuehne, *et al.* Engineering biofunctional in vitro vessel models using a multilayer bioprinting technique. *Sci Rep.* 8(1):10430, 2018.
- ²⁹Shaikh, F. M., A. Callanan, E. G. Kavanagh, P. E. Burke, P. A. Grace, and T. M. McGloughlin. Fibrin: a natural biodegradable scaffold in vascular tissue engineering. *Cells Tissues Organs*. 188(4):333–346, 2008.
- ³⁰Skilton, M. R., L. Boussel, F. Bonnet, S. Bernard, P. C. Douek, P. Moulin, *et al.* Carotid intima-media and adventitial thickening: comparison of new and established ultrasound and magnetic resonance imaging techniques. *Atherosclerosis*. 215(2):405–410, 2011.
- ³¹Stenmark, K. R., M. E. Yeager, K. C. El Kasmi, E. Nozik-Grayck, E. V. Gerasimovskaya, M. Li, *et al.* The adventitia: essential regulator of vascular wall structure and function. *Annu Rev Physiol.* 75:23–47, 2013.
- ³²Xu, Y., Y. Hu, C. Liu, H. Yao, B. Liu, and S. Mi. A novel strategy for creating tissue-engineered biomimetic blood vessels using 3D bioprinting technology. *Materials (Basel)*. 11(9):1581, 2018.
- ³³Zhang, Y., X. S. Li, A. G. Guex, S. S. Liu, E. Müller, R. I. Malini, *et al.* A compliant and biomimetic three-layered vascular graft for small blood vessels. *Biofabrication*. 9(2):025010, 2017.
- ³⁴Zippusch, S., F. Helms, S. Lau, M. Klingenberg, C. Schrimpf, A. Haverich, *et al.* Perfusion promotes endothelialized pore formation in high concentration fibrin gels otherwise unsuitable for tube development. *Int J Artif Organs*. 2020. <https://doi.org/10.1177/0391398820936700>.
- ³⁵Zudaire, E., L. Gambardella, C. Kurcz, and S. Vermeren. A computational tool for quantitative analysis of vascular networks. *PLoS ONE*. 6(11):e27385, 2011.
- ³⁶Zuk, P. Adipose-derived stem cells in tissue regeneration: a review. *ISRN Stem Cells*. 2013:713959, 2013.

Publisher's Note Springer Nature remains neutral with regard to jurisdictional claims in published maps and institutional affiliations.